Renewable and Sustainable Energy Reviews 16 (2012) 2926–2939

Contents lists available at SciVerse ScienceDirect

Renewable and Sustainable Energy Reviews

journal homepage: www.elsevier.com/locate/rser

Hybrid renewable energy systems for power generation in stand-alone applications: A review

Prabodh Bajpai*, Vaishalee Dash

Department of Electrical Engineering, IIT Kharagpur, Kharagpur 721 302, West Bengal, India

ARTICLE INFO

Article history:
Received 13 July 2011
Accepted 5 February 2012
Available online 22 March 2012

Keywords:
Fuel cells
Hybrid renewable energy systems
Photovoltaic

ABSTRACT

It has become imperative for the power and energy engineers to look out for the renewable energy sources such as sun, wind, geothermal, ocean and biomass as sustainable, cost-effective and environment friendly alternatives for conventional energy sources. However, the non-availability of these renewable energy resources all the time throughout the year has led to research in the area of hybrid renewable energy systems. In the past few years, a lot of research has taken place in the design, optimization, operation and control of the renewable hybrid energy systems. It is indeed evident that this area is still emerging and vast in scope. The main aim of this paper is to review the research on the unit sizing, optimization, energy management and modeling of the hybrid renewable energy system components. Developments in research on modeling of hybrid energy resources (PV systems), backup energy systems (Fuel Cell, Battery, Ultra-capacitor, Diesel Generator), power conditioning units (MPPT converters, Buck/Boost converters, Battery chargers) and techniques for energy flow management have been discussed in detail. In this paper, an attempt has been made to present a comprehensive review of the research in this area in the past one decade.

© 2012 Elsevier Ltd. All rights reserved.

Contents

1. Introduction

The rapid industrialization over the past three decades due to globalization, inventions in new technologies and increased household energy consumption of the urban population has resulted in the unprecedented increase in the demand for energy and in particular electricity. This has led to a huge supply–demand gap in the power sector. The scarcity of conventional energy resources, rise in the fuel prices and harmful emissions from the burning of fossil fuels has made power generation from conventional energy sources unsustainable and unviable. It is envisaged that this supply–demand gap will continue to rise exponentially

* Corresponding author. Tel.: +91 9933363474, +91 3222 281752.
E-mail address: pbajpai@ee.iitkgp.ernet.in (P. Bajpai).

1364-0321/$ – see front matter © 2012 Elsevier Ltd. All rights reserved.
doi:10.1016/j.rser.2012.02.009

unless it is met by some other means of power generation. Inaccessibility of the grid power to the remote places and the lack of rural electrification have prompted for alternative sources of energy. The renewable energy resources, such as wind, sun, water, sea and biomass, have become better alternatives for conventional energy resources.

Hybrid Renewable Energy Systems (HRES) is composed of one renewable and one conventional energy source or more than one renewable with or without conventional energy sources, that works in stand alone or grid connected mode [1]. HRES is becoming popular for stand-alone power generation in isolated sites due to the advances in renewable energy technologies and power electronic converters which are used to convert the unregulated power generated from renewable sources into useful power at the load end. The important feature of HRES is to combine two or more renewable power generation technologies to make best use of their operating characteristics and to obtain efficiencies higher than that could be obtained from a single power source. Hybrid systems can address limitations in terms of fuel flexibility, efficiency, reliability, emissions and economics.

A generalized model of HRES is illustrated with a block diagram in Fig. 1, where either one or both of the renewable sources (solar PV/wind) can be used in combination with back up devices, such as FCs, batteries, UCs or DG sets. Solar PV and wind systems are the primary sources of energy. This energy is available in abundance, but is intermittent in nature and site specific. To overcome this drawback, back up energy devices (secondary sources) are introduced into the system to supply the deficit power and to take care of transient load demands. The primary and secondary sources are connected to the dc bus through dc–dc converters to obtain regulated power output from the sources and to maintain a constant voltage at the dc bus. The converters for PV/wind system are usually a cascade of two dc–dc converters, one used for maximum power tracking and the other for voltage regulation. Similarly, dc and ac loads are connected to the dc bus through dc–dc and dc–ac converters respectively. This ensures regulated power supply to the loads throughout operation. The batteries and UCs are connected to the dc bus via bi-directional dc–dc converters for effective charging and discharging. DG sets are connected by means of ac–dc converters. The FC stack and electrolyzer need individual dc–dc converters for regulated power output and conversion.

The entire system has one master controller and several slave controllers for different sources. The master controller operates in close co-ordination with all energy sources and slave controllers. It controls the switching action between the primary and back up energy sources depending on availability of power and prior set control logic. The voltage and current measurements of an individual power source are taken locally by respective slave controller and is relayed back to the master controller at each sampling instant. The slave controller also generates PWM signals for the dc–dc converter under its control and hence monitors the power regulation. The solid black arrows indicate the flow of energy from the sources to the dc bus and from dc bus to loads. The dotted arrow lines indicate the control action and information flow between the sources and controllers. This HRES ensures continuous and effective delivery of power to the loads.

Solar Photovoltaic (PV) and wind energy which are renewable, site-dependent and non-polluting are potential sources of alternative energy. Nonetheless, standalone PV/wind systems can meet the load demand only for the time during which sunshine/cut-in wind speeds are available. Hence, HRES invariably includes backup energy storage systems to meet the load demand at any point of time. The elements of backup energy storage systems are either fuel cell (FC) or battery or diesel generator (DG) or ultra-capacitor (UC) or a combination of these sources. While batteries are most commonly used for this purpose, they typically lose 1–5% of their energy content per hour and thus can store energy only for short period of time [2]. The various possible hybrid system configurations can be designed based on availability of primary energy sources (PV and/or wind) onsite. Backup energy sources are complimentary in nature due to difference in capital and operating costs, power and energy characteristics and fuel flexibility. However, this review is focused mainly on PV based HRES due to space limitations.

PV technology is a relatively new field of renewable energy that is rapidly expanding. The amount of power generated by a PV array depends on the operating voltage of the array and the maximum power point (MPP), which vary with solar insolation and temperature. MPP specifies a unique operating point on PV characteristic at which maximum possible power can be extracted. At the MPP, the PV operates at its highest efficiency. Therefore, many methods have been developed to track the MPP [3]. The output power of the solar module is highly affected by the sunlight incident angle and its efficiency can be improved if the solar module is properly installed at the optimum angle. Chen et al. [4] calculated the optimum installation angle for the fixed solar modules based on the genetic algorithm (GA) and the simulated-annealing (SA) method.

Significant research on economic and environmental aspects of integrating the PV system with DG has been reported [5–8]. The DG backup for PV systems has gained popularity for quite long time as it is capable of supplying electric energy for 24 h, at low capital cost. However, increased fuel prices, intensive maintenance and harmful carbon emissions from DG sets have made them unsustainable and unattractive [9]. Moreover, the whole system efficiency decreases drastically when the DG has to be run lower than the rated output. UCs have also been suggested as back up devices for offering high energy density as compared to ordinary capacitors and high power density than batteries [10,11]. They also have high round trip efficiency (greater than 90%) and can support greater number of charge/discharge cycles.

Over the time, FCs are replacing the DG as an alternative backup energy resource in the integrated PV systems. The major problems associated with FCs are the high cost of the membrane and catalyst as well as fuel availability [12]. However, the combination of the FC and the renewable energy source can provide a multi-fold benefit [13]. First, fossil fuel consumption would be reduced because of higher FC efficiency than DG, and second benefit would be reduction of power losses, since the FC power plant can be placed at or near the load center to take advantage of its low noise and emissions. Another important advantage in using FC is its fuel flexibility. However, the most common fuel used is hydrogen. Hydrogen can be derived from natural gas, ethanol, methanol, biogas, and coal gas, propane, naphtha or other similar hydrocarbons through reforming. This type of hybrid system is particularly useful in spaceship, transportation and stationary applications. Hydrogen prices are likely to drop in future to about double price of natural gas as hydrogen is becoming a commodity. The decisive economical factor is the effective cost per kWh. Today's FCs are already competitive in comparison to DG, offering a huge up-side potential with the expected cost decrease in hydrogen and cost increase in diesel. If the whole system is properly designed, then FC results in reduced maintenance effort and cost compared with a DG [14].

The review article discusses four main aspects in the subsequent sections, i.e. unit sizing and optimization of the HRES, modeling of the major components used in hybrid PV systems with FC, DG, Battery or UC as backup, modeling of power conditioning units, optimal energy flow management and at last the challenges faced by HRES and future trends that can help in improving the system. The sizing and optimization study is essential before setting up or installation of a HRES. It gives a fair idea of the size of the individual components and hence plays an important role in the initial capital investment. The modeling of components is highly significant in understanding the physical mechanisms and power generation ability of the

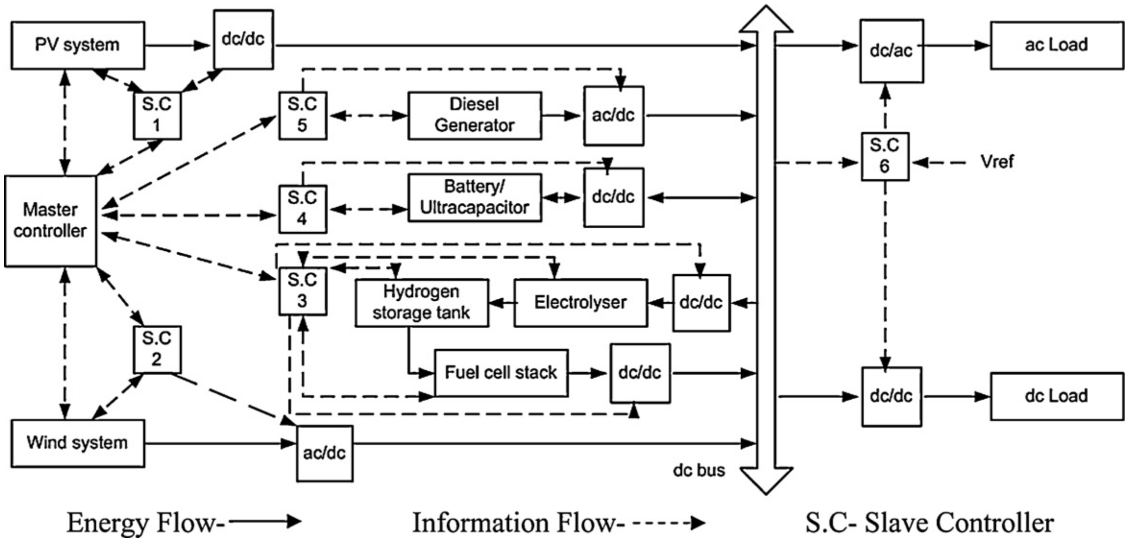


Fig. 1. Generalized model of block diagram of hybrid renewable energy system.

components. It is useful for simulation studies. The optimal energy flow study devises techniques and schemes to operate the system at minimum cost but with high reliability. Lastly, the challenges bring forward the gaps in research areas and the discussion on future trends is vital for improving the overall technology of the HRES.

2. Unit sizing and optimization

Renewable energy sources essentially have random behavior and cannot have accurate prediction. Continuous sunny days give abundant PV power because of which the battery banks or hydrogen tanks are underutilized. On the other hand, cloudy days with continuous rain can discharge the batteries and hydrogen storage tanks well beyond the lower discharge limit. Therefore, the number of PV modules to be installed, the size of the FC, battery bank and hydrogen storage tanks need to be calculated carefully considering all extreme weather conditions. Unit sizing and optimization is basically a method of determining the size of the hybrid system components by minimizing the system cost while maintaining system reliability. Optimum resource management in a hybrid generation system is crucial to achieve acceptable cost and reliability level. These design objectives are usually conflicting with one another and thus a reasonable tradeoff between them is desirable. Over sizing the system components will increase the system cost whereas under sizing can lead to failure of power supply. Thus, sufficient care should be taken to design a reliable system at minimum cost.

A classification chart that groups and classifies the various sizing procedures is illustrated in Fig. 2. This broad classification is based on the availability and non-availability of weather data, such as irradiance, clearness index and wind speed [15]. When weather data is available, conventional sizing approaches are used and are classified on the basis of concept of energy balance and reliability of supply. However, conventional techniques need long term meteorological data for sizing of PV systems, which may not be available in remote isolated sites. Thus, non availability of weather data in remote sites has urged the researchers to look into Artificial Intelligence (AI) techniques, such as Artificial Neural Networks (ANN), Fuzzy Logic (FL), Genetic Algorithms (GA) or a hybrid of such techniques [16].

Conventional sizing methods are in use for more than two decades and give accurate results when actual weather data is available. One of the simple ways of sizing components is based on the concept of energy balance. The daily average available energy from the sun and the daily average load demand are balanced to determine the number of modules needed. The available energy from the sun can be determined from solar irradiance data. Sizing based on energy balance takes into consideration the path losses and efficiencies of the source, converters and controllers. Li et al. [17] proposed an algorithm to determine the minimal system configuration using an iterative technique based on energy balance. The optimal sizes of the system components for a hybrid PV/FC/Battery system producing onsite hydrogen were determined in [18]. Sizing of batteries were done by carefully choosing the days of autonomy, a vital parameter in battery sizing. FC and electrolyzer sizing were done taking marginal safety.

Some of the sizing procedures in the literature consider the reliability of electricity supply as an important factor. This reliability is determined by estimating the loss of load probability (LOLP) which is the ratio between estimated energy deficit and the energy demand over the total time of operation [15]. Other similar concepts are loss of power probability (LOPP), loss of power supply probability (LPSP) and load coverage rate (LCR). Such sizing techniques are used in applications where a high degree of reliability is required. Ardakani et al. [19] used a reliability index called equivalent loss factor (ELF) for optimizing the size of the components in a hybrid wind/PV/Battery system. Xu et al. [20] proposed a strategy to minimize the total system cost subject to the constraint of LPSP using GA. Moriana et al. [21] also used LPSP as a reliability index for sizing the storage unit in a wind/PV system. Nelson et al. [22] considered an LPSP less than or equal to 0.0003 which corresponds to a loss of power of 1 day in 10 years for sizing the PV modules and hydrogen tanks in a wind/PV/FC system.

In remote inaccessible sites, weather data collection is difficult. Hence researchers devised AI based techniques to size the PV systems. Mellit et al. [16] discussed various AI methods for sizing of PV systems. Some of the AI techniques are ANN, FL, GA or a hybrid of such methods. These methods can tolerate certain degree of error in the input data; generate fast results once trained from examples and model complex non-linear processes with ease. ANN is a collection of interconnected processing units where each incoming connection has an input value and a weight attached to it. The output is a function of the summed units. ANNs can then be trained

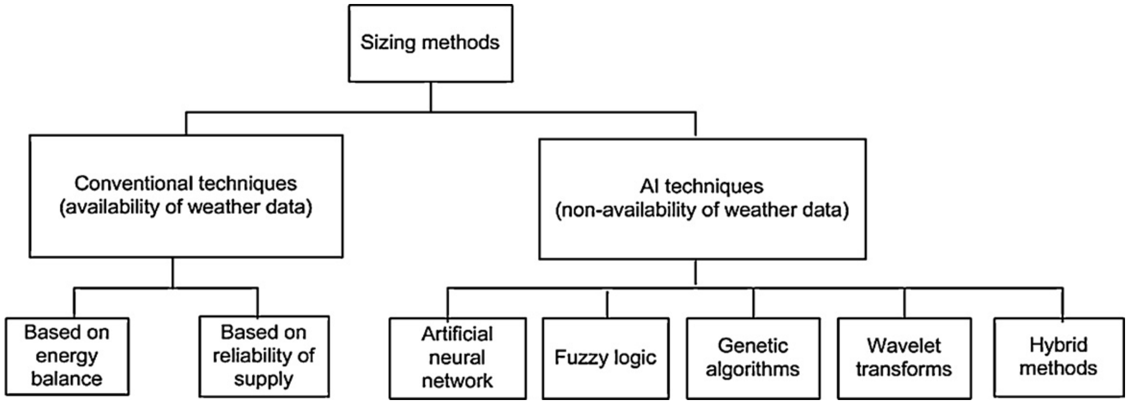


Fig. 2. Classification of hybrid system sizing methods.

Table 1
Artificial intelligence (AI) techniques used in sizing of HRES.

Sl no.	AI technique used & references	Brief description
1.	Genetic Algorithms (GA) [20,24,25]	Optimal sizing of standalone hybrid wind/PV systems and wind/PV/DG systems
2.	Artificial neural network (ANN) [23,26]	Sizing PV systems using adaptive ANN
3.	Hybrid methods	
	a) Combination of neural network and wavelet transform [27]	Sizing of standalone PV system using neural network and wavelet techniques
	b) Combination of neuro-fuzzy and GA [28]	Using neuro-fuzzy and GA for sizing standalone PV systems

with respect to data sets, and once trained, new patterns may be presented to them for prediction or classification. FL allows the application of a ‘human language’ to describe the problems and their fuzzy solutions. When input parameters are highly variable and unstable, fuzzy controllers can be used as they are more robust and cheaper than conventional PID controllers. Hybrid methods use a combination of two or more AI techniques for sizing the system. Mellit et al. [23] considered the latitude and longitude of the site as inputs and estimated two outputs based on an ANN model for sizing the PV system. The output parameters allowed successful sizing of the number of PV modules and batteries with a relative error less than 6%. Similar applications of various AI techniques in sizing and optimization of HRES are listed in Table 1.

Sizing of the components is generally accompanied by optimizing the system components or other parameters, such as investment cost, output energy cost or consumption of fuel [29]. Optimization is generally carried with the objective of minimizing the Net Present Cost (NPC) or by minimizing the Levelized Cost of Energy (LCE) [30]. Wang and Singh [31] proposed a constrained mixed-integer multi objective particle swarm optimization (PSO) method to minimize the system cost and simultaneously maximize the system reliability. The unit sizing and optimization by minimizing the NPC using HOMER for a hybrid PV-Wind-Diesel-Battery system and hybrid PV-Diesel-Battery system has been carried out in [32] and [33], respectively. Ashok [34] used non-linear constrained optimization techniques to minimize the annual operating cost for a hybrid PV-Wind-Diesel-Battery system including a micro-hydro. The renewable energy fraction was calculated to be 100% and the need for DG was hence eliminated. Several simulation tools are readily available today in order to model, size and optimize the hybrid system. An overview of such simulation and/or optimization tools is discussed in [29,30]. A brief description of a few popular simulation tools is listed in Table 2.

3. Modeling of hybrid renewable energy systems (HRES) components

3.1. *Modeling of solar photovoltaic*

A solar photovoltaic (PV) system converts the solar energy directly into electricity. The smallest unit of this system is the solar cell. Cells are then arranged in the module which is further connected in series and/or parallel fashion to form arrays. The dc electricity produced at the terminals of the arrays can be used in a variety of applications, such as dc motors or lighting systems. The PV system is highly non-linear as can be evident from its current vs voltage (I–V) characteristics shown in Fig. 3 [40]. It exhibits either current source or voltage source behavior depending on the operating point lying on the left or right of P, respectively [40]. At maximum power point (MPP), product of voltage (V_{mp}) and cur-

Table 2
Simulation tools and their features used in HRES.

Sl no.	Simulation tool	Developed by, references	Brief description
1.	HOMER	NREL [35]	Simulation and sizing of HRES based on optimization of NPC, considering wind turbines, PV modules, batteries, small hydro and many other components
2.	HYBRID2	NREL and University of Massachusetts [36]	Long term performance and economic analysis of HRES
3.	PV SOL	Valentin Energy Software [37]	Designing, planning of both stand-alone and grid-connected systems and analysis of electricity consumption and its costs
4.	RAPSIM	MUERI in a project funded by ACRE [38]	Simulation of HRES including PV, wind, diesel generators
5.	TRNSYS	Solar Energy Laboratory, University of Wisconsin-Madison [39]	Simulation of solar thermal systems, solar PV, wind and several other components without optimization

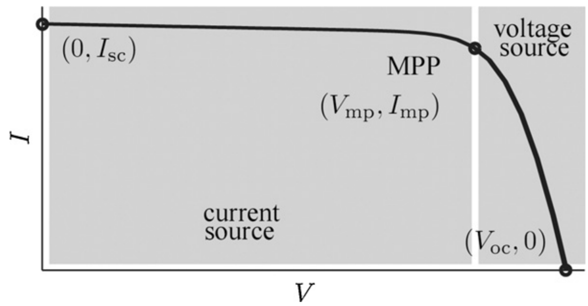


Fig. 3. *I–V* characteristics of a PV module.

rent (I_{mp}) is maximum. I_{sc} and V_{oc} are open circuit voltage and short-circuit current, respectively.

Modeling PV arrays is one of the key components in the analysis of PV systems' performance. There are several mathematical models describing PV behavior under external influences, such as temperature and solar irradiance. Hence it is necessary to classify the existing models to simplify the study of PV arrays. Broadly these models can be categorized as electrical and thermal models. Electrical models give the relationship between the PV output voltage and current based on certain parameters such as the reverse saturation current of diode and losses occurring in the series and parallel resistances. The thermal models, however, take into consideration the effect of operating temperature in modeling. This is determined by energy balance concept, i.e. the solar energy absorbed by a module is converted partly into thermal energy and rest into electrical energy. The increase in cell temperature mainly due to increasing solar insolation throughout the day is calculated depending on the heat loss coefficients and cell efficiency.

3.1.1. *Electrical models*

A simple equivalent circuit model for a PV cell consists of a diode in parallel with an ideal current source. The ideal current source delivers current in proportion to the solar flux to which it is exposed. A more accurate model of a PV cell [41] considers the effect of series (R_s) and parallel resistance (R_{sh}) as shown in Fig. 4. This equivalent circuit holds good for a cell, a module or even an array. In a practical PV cell, a series resistance is offered by the semiconductor material, the metal grid, metal contacts and current collecting bus. These resistive losses are lumped together as a series resistor (R_s). Its effect becomes very conspicuous in a PV module that consists of many series-connected cells, and the value of resistance is multiplied by the number of cells. Similarly a certain loss is associated with a small leakage of current through a resistive path in parallel with the intrinsic device. This can be represented by a parallel resistor (R_{sh}). Its effect is much less conspicuous in a PV module compared to the series resistance, and it will only become

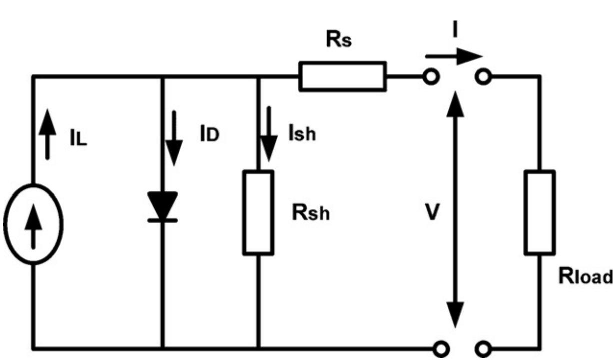


Fig. 4. Electrical equivalent circuit of a single diode model of a PV cell considering the effect of series and shunt resistances.

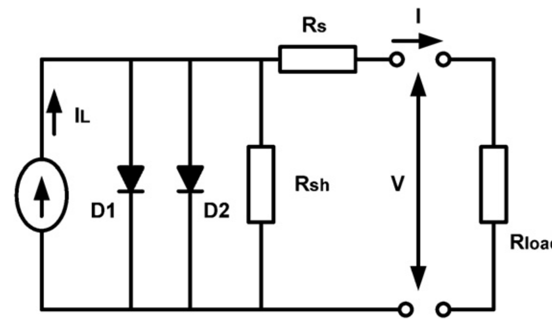


Fig. 5. Electrical equivalent circuit of a two diode model of a PV cell.

noticeable when a number of PV modules are connected in parallel for a larger system [42].

The relationship between voltage and current [41] for the equivalent circuit of the PV cell (Fig. 4) considering both the series and shunt resistances is

$$I = I_L - I_D - I_{sh} = I_L - I_o \left\{ \exp\left[\frac{V + IR_s}{a}\right] - 1 \right\} - \frac{V + IR_s}{R_{sh}} \quad (1)$$

where I_L is the PV cell generated current, I_o is the reverse saturation current, I_D is the diode current, I_{sh} is the shunt current, R_s is the series resistance, R_{sh} is the shunt resistance, a is the curve fitting parameter, I is the load current and V is the load voltage. This is the single diode model considering both R_s and R_{sh} or it is sometimes known as the five parameter model as it depends on I_L, I_o, R_s, R_{sh} and a. Few authors have neglected the value of R_s [43] and R_{sh} [44] during modeling. This converts the five parameter model to a four parameter one.

While modeling a PV module under standard test conditions (STC) the values of I_L, I_o, a and R_s [41] can be calculated from the expressions in the following equations. Eqs. (2–5) below have neglected the value of R_{sh}.

$$I_{L,ref} = I_{sc} \quad (2)$$

$$I_{o,ref} = I_{L,ref} \exp\left(\frac{-V_{oc}}{a}\right) \quad (3)$$

$$a_{ref} = \frac{\mu_{V,oc} T_{c,ref} - V_{oc,ref} + e_{gap} N_s}{(\mu_{I,sc} T_{c,ref} / I_{L,ref}) - 3} \quad (4)$$

$$R_s = \frac{a \ln(1 - (I_{mp}/I_L)) - V_{mp} + V_{oc}}{I_{mp}} \quad (5)$$

where I_{sc} is the short circuit of the module, V_{oc} is the open circuit voltage of the module, N_s is the number of cells in series in a module times the number of modules in series in an array, $\mu_{I,sc}$ is the temperature coefficient of the short circuit current, $\mu_{V,oc}$ is the temperature coefficient of the open circuit voltage, e_{gap} is the band-gap energy of the material, I_{mp} and V_{mp} are the current and voltage at maximum power point, respectively, and T_c is the cell temperature. These values are usually given in the datasheet of the PV modules supplied by the manufacturer. As temperature and insolation influence the electrical output from PV module, the values of I_L, I_o, a can be calculated at any temperature and irradiance [41]. However, in Eq. (5) the variation of R_s with respect to temperature is neglected.

Recombination in the depletion region of PV cells provides non-ohmic current paths in parallel with the intrinsic PV cell [45]. This is represented by the second diode (D2) in the equivalent circuit [46] of a PV cell as shown in Fig. 5. The two diode model [47,48] provides improved accuracy and is applicable mainly for solar cells made of polycrystalline silicon. An advanced three diode model is proposed in [49] for multi-crystalline silicon solar cells considering the influence of grain boundaries and large leakage currents through the cell periphery.

Electrical models	Thermal models
- single diode model [41] - two diode model [46,47,48] - three diode model [49] - models considering only R_s [43] - models considering only R_{sh} [44]	- model based on U_L (overall heat loss coefficient) [41,50] - model based on U_L and C_t (thermal capacitance) [50]

Fig. 6. Classification of solar PV models.

3.1.2. Thermal models

The performance of a PV module strongly depends on its operating temperature. The incoming solar energy absorbed by a module is partly converted into thermal energy [41] that is dissipated by a combination of conduction, convection and radiation. The cell temperature depends on the ambient conditions and also on the operation of the PV module. For best operation, minimum possible temperature is preferred. Energy balance on unit area of a PV module, cooled by losses to the surroundings is represented as [50]

$$C_t \frac{dT_c}{dt} = \tau\alpha G_T - \eta_c G_T - U_L(T_c - T_a) \tag{6}$$

where C_t is the thermal capacitance of PV module, G_T is irradiance, T_a is ambient temperature, T_c is cell temperature, U_L is overall heat loss coefficient, η_c is efficiency of PV cells and $\tau\alpha$ is the transmittance-absorption product of PV cells. If only U_L is considered, T_c is determined as in Eq. (7). If both U_L and C_t are considered, Eq. (6) reduces to a linear, first order, non-homogeneous differential equation represented as Eq. (8). The solution of Eq. (8) is given as in Eq. (9).

$$T_c = T_a + \left(G_T \frac{\tau\alpha}{U_L}\right)\left(1 - \frac{\eta_c}{\tau\alpha}\right) \tag{7}$$

$$\frac{dT_c}{dt} + aT_c - b = 0 \tag{8}$$

$$T_c(t) = \left(T_{c,init} - \frac{b}{a}\right)\exp(-at) + \frac{b}{a} \tag{9}$$

where constants a and b are given by

$$a = \frac{U_L}{C_t} = \frac{1}{\tau_t} \tag{10}$$

$$b = \frac{(\tau\alpha - \eta_c)G_T + U_L T_a}{C_t} \tag{11}$$

where t is time in seconds, $T_{c,init}$ is the temperature of cell at initial conditions and τ_t is thermal time constant for PV module.

Based on the literature review covered in the present work a broad classification of the PV models and their variants is illustrated in Fig. 6. Several variants of electrical and thermal models available in the literature are already discussed in detail in previous subsections.

3.2. Modeling of fuel cell

Fuel cell (FC) is an electrochemical energy conversion device that converts the chemical energy of a fuel directly into electricity. Depending on the type of electrolyte used several types of FCs, such as Proton Exchange Membrane (PEM) FC, Alkaline FC, Molten Carbonate FC and Solid Oxide FC, have been developed [51]. Substantial amount of research has been made regarding the use of fuel cells as alternative sources of power for transportation and stationary power generation. Among all types of fuel cells, PEM is very promising owing to its low temperature operation and quick start up. Hence, only PEM fuel cell models are reviewed in the present work.

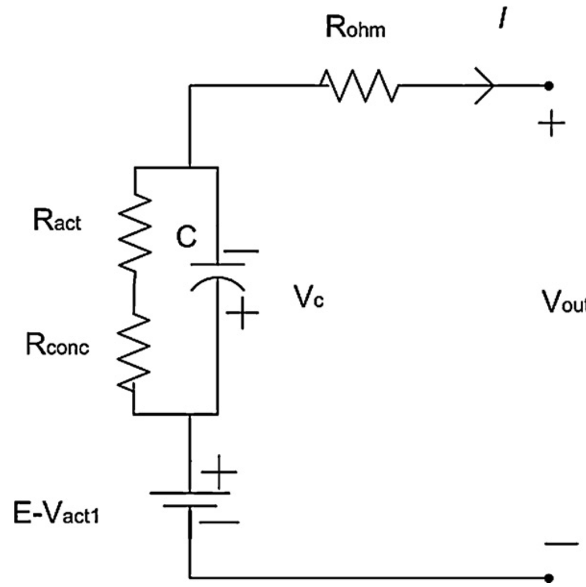


Fig. 7. Electrical equivalent circuit of a fuel cell.

The electrical equivalent circuit of a FC [52] is shown in Fig. 7. The FC terminal voltage is less than that due to the activation, ohmic and concentration voltage drops occurring inside the FC [53]. The activation voltage drop is due to the energy required to initiate the chemical reaction associated with sluggish electrode kinetics. The ohmic losses occur in the cell because of resistance to the flow of ions in the electrolyte, electrons in the outer circuit and contact resistance. There is a further drop in potential at higher current densities due to depletion of reactants at higher currents and is known as concentration polarization. In addition, two oppositely charged layers are formed across the boundary between the electrodes and electrolyte.

This double charge layer behaves as a capacitor and tends to store charge. Its charge storage ability adversely affects the dynamic response. The capacitor is represented in parallel to the activation and concentration voltage drops as it does not immediately follow the current as the ohmic voltage drop does due to the slow electrochemical reactions in the FC.

The FC output voltage can hence be given as [52]

$$V_{out} = E - V_{act1} - V_C - V_{ohm} \tag{12}$$

where E is the internal voltage developed across the FC, V_{act1} is the temperature dependent term of activation voltage drop, V_C is the voltage developed across the capacitor and V_{ohm} is the voltage drop due to ohmic losses.

The voltage E developed over a single cell, ideally described by the Nernst equation is given as

$$E = E_o + \frac{RT}{2F}\ln\left(\frac{P_{H_2}P_{O_2}{}^{1/2}}{P_{H_2O}}\right) \quad (13)$$

where E_0 is the standard potential of the hydrogen/oxygen reaction (about 1.229 V), R is the universal gas constant, F is Faraday's constant and T is the gas temperature. P_{H_2} is the partial pressure of hydrogen available at the anode; P_{H_2O} and P_{O_2} are partial pressures of water and oxygen, respectively, at the cathode.

$$V_{act1} = \eta_0 + (T - 298)a \quad (14)$$

where η_0 and a are empirical constants.

$$V_C = \left(I - C\frac{dV_C}{dt}\right)(R_{act} + R_{conc}) \quad (15)$$

where I is the load current, C is the internal capacitance and the equivalent resistance R_{act} and R_{conc} represents activation and concentration voltage drop, respectively.

$$V_{ohm} = IR_{ohm} \quad (16)$$

where R_{ohm} is the equivalent resistance representing ohmic voltage drop in the FC.

Fuel cell modeling can be broadly classified into three categories [54] shown in Fig. 8. Analytical models are reported by Standaert et al. [55,56], make simple assumptions to arrive at an approximate V–I density relationship and hence do not give an actual picture of water transport processes occurring in the cell. In semi-empirical modeling, the theoretically derived differential and algebraic equations combine with empirically determined relationships. FC models used in HRES are mostly one-dimensional semi-empirical models [57,58]. The mechanistic models are based on electrochemical, thermodynamic and fluid dynamic equations and, in general, have high level of details, requiring the knowledge of parameters that are very difficult to be obtained, such as transfer coefficients, humidity levels, membrane, electrode and active catalyst layer thicknesses. A one-dimensional, steady state, isothermal model with water transport, reactant species transport is presented by Bernardi and Verbrugge [59,60].

A review of existing models of PEMFC reveals that substantial research has been done to study the steady state behavior and dynamic behavior of FCs. The dynamic aspects in the behavior of FCs are analyzed and discussed in detail [61,62]. Electrochemical, thermal and a combination of both to form a transient model are discussed in these articles to study the effect of change in load, operating temperature and gas flows. Sharifi Asl et al. [63] discussed a model to study both the steady state and dynamic behavior by a lumped parameter model. It also takes into account the double charge layer phenomena in FCs [52]. There are a few review articles giving an overview of existing mathematical models of PEMFC, classifying and comparing some of them [54,64].

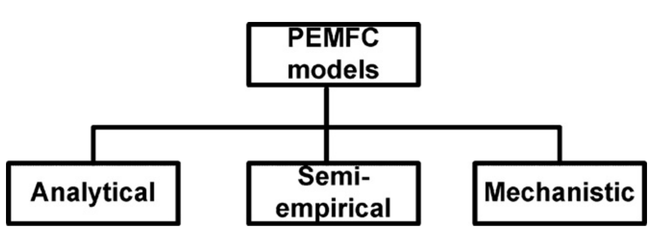


Fig. 8. Classification of PEMFC models.

3.3. Modeling of electrolyzer

The fuel needed for power generation in FCs is hydrogen. But despite of its abundance in atmosphere, hydrogen is not freely available and occurs mostly in combination as molecular compounds. Separation of hydrogen from these compounds is an energy intensive process. Removal of hydrogen from fossil fuels is easy as these fossils are at a higher energy state. Such a process known as reforming is however polluting in nature. Separation of hydrogen from water needs more energy than the reforming process, but does not release any pollutant. The process of extracting hydrogen from water is called electrolysis and is used in an electrolyzer.

In the process of electrolysis, the water molecules are decomposed into their constituent elements, i.e. water and oxygen. An electrolyzer is as series of cells each containing a positive and negative electrode [52]. The electrodes are immersed in water which is made electrically conductive by adding alkaline potassium hydroxide to furnish the hydroxyl ions (OH^-). Hydrogen and oxygen gases are produced at cathode and anode, respectively. The rate of hydrogen generation depends on the current density. A simple equivalent circuit [52] for an electrolyzer is shown in Fig. 9. $V_{rev,cell}$ is the internal electrolyzer cell voltage, V_{cell} and I are the input dc voltage and current to the electrolyzer, and the nonlinear temperature and current dependent resistor represents the internal losses. Hence, the internal voltage for each cell is expressed as

$$V_{cell} = V_{rev,cell} + V_{drop,cell} \quad (17)$$

where $V_{drop,cell}$ corresponds to the voltage drop across the nonlinear current and temperature dependent resistor block. A more detailed model considering parasitic losses is discussed in [52].

Lebbal and Lecoeuche [65] proposed another electrical model for the electrolyzer. This model more accurately represents the potential drops observed in the electrolyzer cells. These voltage drops correspond to a reversible drop V_{rev}, activation drop V_{act}, propagation drop V_{prog} and drop due to ohmic losses V_{ohm}. Hence the applied voltage U can be expressed as

$$U = V_{rev} + V_{act} + V_{prog} + V_{ohm} \quad (18)$$

where V_{rev} is the cell potential when current is nil and is expressed as

$$V_{rev} = V_0 + \frac{RT}{2F}\ln\left(\frac{P_{H_2}P_{O_2}^{1/2}}{a_{H_2O}}\right) \quad (19)$$

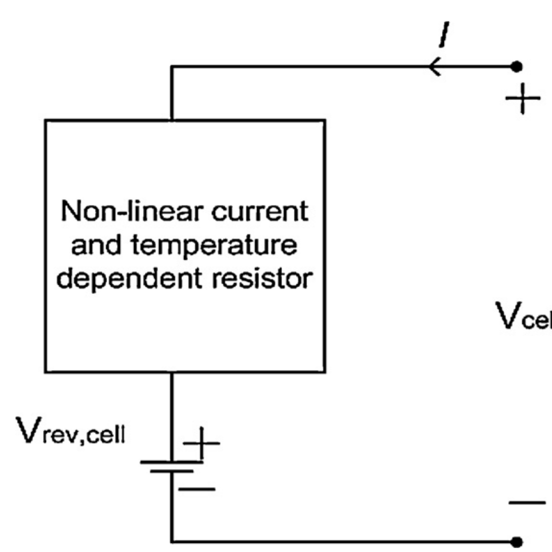


Fig. 9. Electrical equivalent circuit of an electrolyzer.

where R, F, V_0 and a_{H_2O} are the universal gas constant, the Faraday's constant, the standard reversible voltage and the water activity, respectively. P_{H_2}, P_{O_2} and T are the partial pressures of hydrogen and oxygen and gas temperature, respectively.

V_{act} is the potential drop due to the electrochemical kinetic behavior and is expressed as

$$V_{act} = \frac{RT}{\alpha nF} \ln\left(\frac{I}{I_0}\right) \tag{20}$$

where α, I_0 and n are the transfer co-efficient, exchange current and number of electrons participating in the reaction, respectively.

The propagation of gases affects the partial pressures and chemical reaction velocity and causes a potential drop, V_{prog} expressed as

$$V_{prog} = \frac{RT}{\beta nF} \ln\left(1 + \frac{I}{I_{lim}}\right) \tag{21}$$

where β and I_{lim} are the constant coefficient and the diffusion limit current, respectively.

The ohmic loss V_{ohm} occurs mainly due to the resistance of polymer membrane, R_{mem} and hence V_{ohm} is given as

$$V_{ohm} = R_{mem} I \tag{22}$$

Moschetto et al. [66] proposed an electrolyzer model based on its energy efficiency (η_{Estack}) and defined it as the ratio between the hydrogen produced in watts and the dc power supplied to the electrolyzer.

$$\eta_{Estack} = \frac{HHV_{H_2} Q_{H_2}}{V_{stack} I_{stack}} \tag{23}$$

where HHV_{H2} is the hydrogen high heating value, Q_{H_2} is the hydrogen flow, V_{stack} is the stack voltage and I_{stack} is the stack current.

Jalilzadeh et al. [67] presented an electrolyzer model in a hybrid PV-FC system based on the availability of hydrogen in terms of power difference and is expressed as

$$SOC_{elec} = \int (P_{elec} \times \eta_{elec})\,dt - \int \frac{P_{FC}}{\eta_{FC}} \tag{24}$$

where $P_{elec} = P_{PV} - P_{LOAD}$, P_{PV} is the power generated by the solar PV array, P_{LOAD} is the power demand by the load, P_{FC} is the power generated by the fuel cell stack, η_{elec} and η_{FC} represent the efficiency of electrolyzer and FC, respectively.

3.4. Modeling of hydrogen tanks

Hydrogen gas poses a great challenge not only in its extraction but also in its storage. The low density of hydrogen gas and low boiling point of liquid hydrogen makes it difficult to store hydrogen either in gaseous or liquid form. Therefore, for all practical purposes, hydrogen gas is either stored as a high pressure gas or as a liquid cooled down to cryogenic temperatures or as metal hydrides where hydrogen gas bound to certain metal.

Mathematical models relating pressure of stored hydrogen gas, efficiency and rated power of the compressors are discussed in [17,68]. Zhou and Francois [69] represented the pressure of stored hydrogen gas using Van der Waals equation of state for real gases as

$$p_{sto} = \frac{RT_{sto}}{V_{sto}} m_{sto} \tag{25}$$

where T_{sto} is the gas temperature, V_{sto} is the storage tank volume, m_{sto} is the net flow rate of hydrogen into the tank and R is the universal gas constant.

Mathematical models for hydrogen storage in metal hydride tanks are discussed in [70,71]. Zini and Tartarini [72] presented a model of hydrogen storage in the process of physisorption (physical adsorption) on activated carbon in a wind-hydrogen hybrid system.

3.5. Modeling of ultra-capacitor

An ultra-capacitor (UC) also called as an electrochemical double layer capacitor [73] is a low voltage energy storage device similar to a battery but exhibiting an extremely high capacitance value [74].

UCs have high power density, low series resistance, high efficiency, large charge/discharge capacity and low heating losses [75]. These deep-discharge capacitors with a fast response are suitable for operation over a wider range of temperature [76]. However the terminal voltage of an UC decreases with decreasing state of charge (SOC) and rate of decrease depends on the load current. Seventy-five percent utilization of the UC causes a drop in the terminal voltage to about 50% of the rated value. Thus for incorporation and effective utilization of these devices in HRES, a dc–dc converter should be used to interface the device with the dc bus to maintain the dc bus voltage [75].

Several models for effective representation of UCs have been suggested in the literature [76] and electrical equivalent circuits of four models are shown in Fig. 10. The choice of the model depends upon the specific application. Though the classical equivalent circuit model (Fig. 10a) is only a first order approximation, in comparison to the others it is simpler to represent or measure its parameters and is mostly used in HRES study [10,73,77].

The classical equivalent circuit comprises of three components [78]: (i) Equivalent Series Resistance (ESR) which represents the voltage drop and the loss due to internal heating during the charging/discharging process, (ii) Equivalent Parallel Resistance (EPR) which represents the effect of leakage current or self discharging and only affects the long term energy storage performance and (iii) Capacitance (C) produced due to the double layer effect. Research shows that the variation of capacitance with voltage is only 10% and very less affected by charging rate [75]. So, it can be assumed to remain constant during the entire period of operation.

UCs are mainly used with FCs in PV or wind energy systems. It improves the dynamic behavior of the hybrid system to load variations due to its fast response compensating for the slow dynamics of the FC. It also helps in reducing the FC system size and peak power shaving and therefore reduces the initial cost of the system. In all such applications the dynamic behavior being of more importance, EPR can be neglected [78]. The total usable energy from an UC is expressed as [10,77]

$$E_{use} = \frac{1}{2} C_{total} (V_i^2 - V_f^2) \tag{26}$$

where $C_{total} = n_p C/n_s$ and C is the capacitance, n_s is the number of UCs connected in series in each string to meet the rated voltage at the dc bus and n_p is the number of such strings connected in parallel to achieve the required storage capacity. V_i is the terminal voltage of the capacitor bank at rated SOC and V_f is the minimum voltage obtainable after discharging the capacitor limited by the dc–dc converter specification [78].

3.6. Modeling of battery

Battery is a storage device essential for storing electrical energy for maximum utilization of intermittent renewable resources. The lead-acid battery which is often used in HRES is complex, nonlinear device controlling operational states of the system. The energy conversion during charging/discharging of the battery takes place with the following reversible reaction:

$$Pb + PbO_2 + 2H_2SO_4 \underset{\text{charging/discharging}}{\longleftrightarrow} 2PbSO_4 + 2H_2O \tag{27}$$

Modeling of lead-acid batteries for real time analysis of HRES must account for the dependence of battery parameters on (i) state of charge, (ii) battery storage capacity, (iii) rate of charge/discharge,

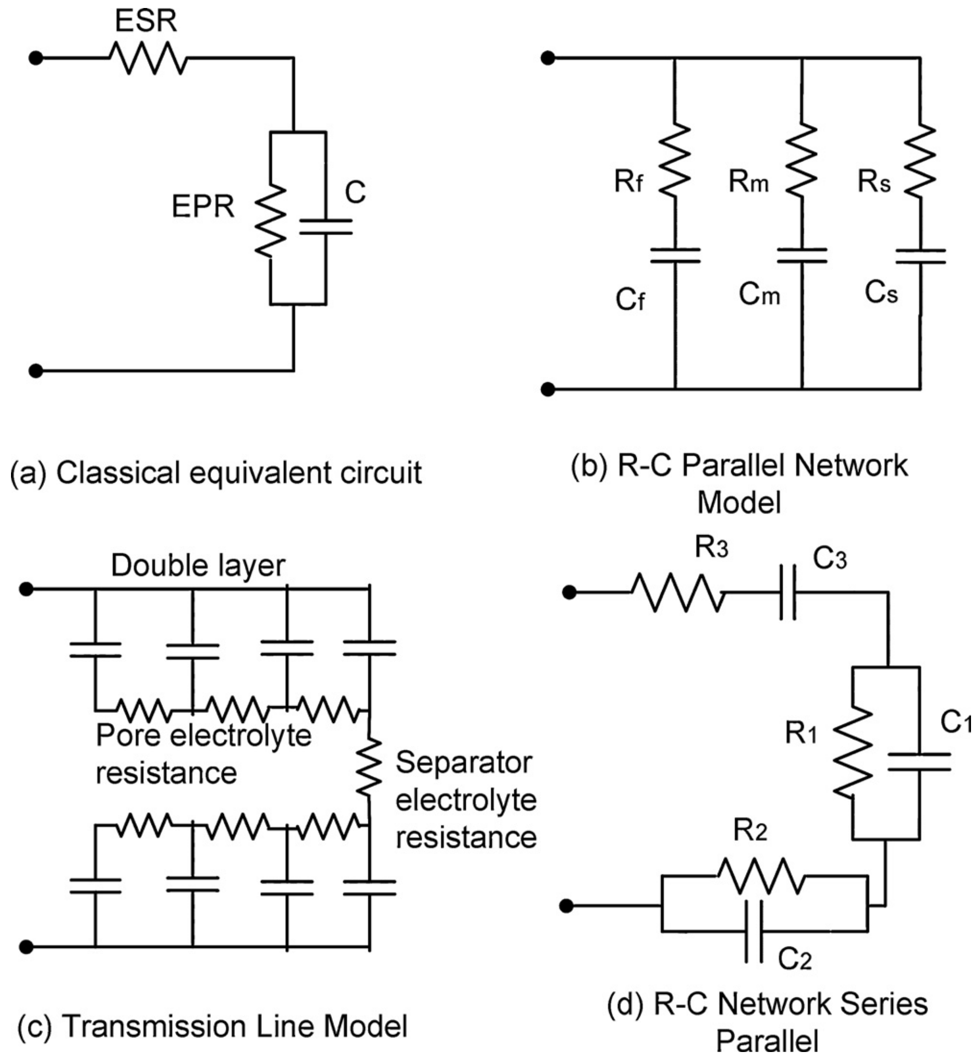


Fig. 10. Electrical equivalent circuit models for ultra-capacitor.

(iv) ambient temperature, (v) life and other internal phenomenon, such as gassing, double layer effect, self discharge, heating loss and diffusion. The equivalent circuit representation of battery as suggested in [79,80] is shown in Fig. 11.

The battery circuit parameters are as follows:

The internal resistance of the battery representing the voltage drop and heating loss is a function of the battery SOC. It remains constant up to 90% rated SOC and then increases exponentially. The charging resistance R_{ich} and the discharging resistance R_{idch} are different in their values.

- R_{dl} and C_{dl} represent the double layer effect occurring due to distribution of ions in the electrolyte in the vicinity of activated electrodes.
- R_d and C_d represent the capacitive effect of the diffusion layers with oppositely charged ions on either side of the electrolyte. Its time constant is much larger than the time constant due to double layer effect. C_b represents the battery capacity in watts.
- With respect to time, as the battery is being charged with a voltage V_{bat} and current I_{bat}, gas resistance R_g decreases exponentially and the gas current I_g increases exponentially. Therefore,

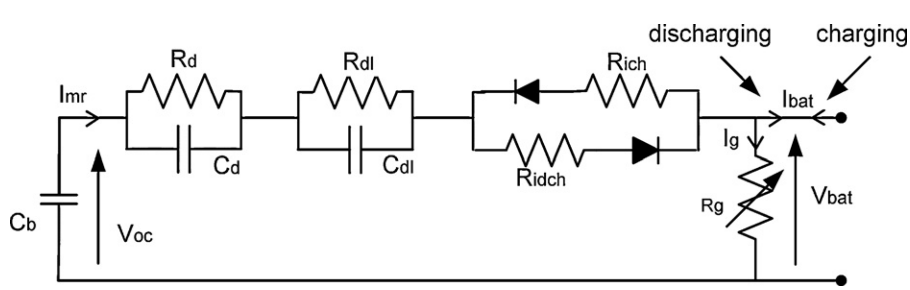


Fig. 11. Electrical equivalent circuit of battery.

a portion of the input energy is spent in producing hydrogen and oxygen and the main reaction current (I_{mr}), which converts electrical energy to chemical energy, decreases correspondingly. Finally complete charging current I_{bat} becomes the gassing current I_g. At this stage, further increment in the battery open-circuit voltage (V_{oc}) is not possible.
- The present SOC is given by the ratio of the ampere hour remaining in battery to rated ampere hour. This along with specific gravity is used for calculating V_{oc} empirically and R_i from experimental data, thus giving an accurate representation for determining battery terminal voltage (V_{bat}).

Battery sizing in a HRES is mostly done on the basis of days of autonomy for which the storage is required to serve the entire load in the absence of power from the other sources of energy [81]. The battery capacity can be calculated in terms of days of autonomy or according to the following expression [82,83]:

$$B_r = \frac{bE_{acload}}{(DOD_{max})\eta_i c_t} \quad (28)$$

where E_{acload} is the total ac load on system in ampere-hour, η_i is the inverter efficiency, DOD_{max} is the maximum allowable depth of discharge, c_t is the temperature correction factor as allowable DOD decreases with decrease in temperature. However, high DOD decreases battery life [84].

In HRES, the mode of operation of battery (i.e. charging or discharging) is dependent on the renewable energy source availability and the load demand. The model required for sizing and economic study is based on an energy balance of battery and subjected to maximum–minimum bounds on the storage state variable to prevent gassing and over-discharging [85–87]. The SOC at any instant ($t+\Delta t$) is given as [88].

$$SOC(t+\Delta t) = SOC(t)(1-\delta) + I_{bat}(t)\Delta t \eta_{bat} \quad (29)$$

where δ is the self discharge coefficient, I_{bat} is the battery current (charge/discharge) and η_{bat} is the battery coulomb's efficiency.

3.7. Modeling of diesel generator

The renewable energy systems have intermittent output characteristics and are integrated with conventional power sources to deliver a steady power output. In various HRES, DG acts as this steady source of power. The DG systems are designed to supply the load and also charge the storage device (say battery), if the renewable energy source along with battery is unable to supply the load. Proper energy balance is required for optimum system operation as the consumption of fuel is proportional to the power being supplied by the DG [84,88].

$$\text{Consumption per hour} = AP_g + BP_{ng} \quad (30)$$

where P_g and P_{ng} are the power generated and nominal power of the DG while A and B are coefficients of the consumption curve in kWh. The DG efficiency is expressed as [89]

$$\eta_{dg} = \eta_t \eta_{mechanical} \eta_{electrical} \quad (31)$$

where η_t is the indicated thermal efficiency that accounts for heat loss in the DG, $\eta_{mechanical}$ corresponds to the frictional losses in moving parts of DG and $\eta_{electrical}$ corresponds to the losses in the alternator. The product of η_t and $\eta_{mechanical}$ is called as brake thermal efficiency. The overall DG efficiency varies with amount of power generated by it and therefore they are operated at around 80–100% of their rated power or may even be controlled to operate in constant power delivery mode [86,87,90]. The DG should have limited operation time to reduce wear and tear [86] as the life of DG is inversely proportional to the energy supplied by it [81].

With the incorporation of some DGs, transient stability issue also surfaces. Since one generator must remain in synchronism with other generators and as well maintain the terminal voltage according to the operational strategy, the speed governor and voltage regulator form an integral part of the DG system. The low frequency transients following a sudden contingency or fault have to be observed. Dynamic study of HRES requires the detail modeling [91] of alternator with state variables in d–q axis [92]; mechanical system with torque balance equation in terms of system parameters (moment of inertia and damping coefficient), speed governor and control mechanism. The d–q axis transformation of the machine state variables allows the dynamic equations to be independent of time varying inductances.

3.8. Modeling of power conditioning units

Due to the high capital cost and requirement of large installation area, it is highly necessary to optimize the performance of the PV modules. Maximum amount of energy should be extracted from the PV array. This can be achieved in two broad ways. One through adjusting the tilt angle of the PV array so that it receives maximum amount of solar insolation. The other is through power electronic control where the operating point of the PV module is adjusted to operate near the MPP. The tilt angle adjustment can be done manually or through a combination of sensors, gears and motors in a solar tracking system.

Solar tracking system can be broadly classified as single-axis tracking, two axis tracking and bi-annual tracking. Single-axis trackers track the sun on a daily basis from east to west. Two-axis trackers track the sun both from east to west on a daily basis and from north to south on an annual basis. Bi-annual tracking is a manual adjustment of the PV module tilt angle twice in a year. It provides a small increase in solar energy received on the module at very low cost and least maintenance. A review of such tracking mechanisms and their implementation is presented in [93] and bi-annual tracking mechanism implementation is discussed in [94].

Electronic control is done based on maximum power point tracking (MPPT) algorithm through sophisticated power electronic converters. Tracking through power electronic converters bring the operating point of the PV close to the MPP. An MPPT algorithm is commonly applied in the converters to maximize the power drawn from PV modules under varying atmospheric conditions. This is to ensure that the best use of the PV array is made in producing clean electricity. It is important in solar power systems because it reduces the PV array cost by decreasing the number of solar modules needed to obtain the same power output.

When a PV array is directly connected to a load, the system operating point will be the intersection of the I–V curves of the PV array and the load. Under most conditions, this operating point is not at the PV array's maximum power point (MPP). In principle, MPPT algorithm sets a reference value in the converter that interfaces the PV array to an electrical load. The reference is chosen so that the converter draws the current or imposes the voltage that operates the PV module at or near the maximum power point (MPP) for the prevailing irradiance and temperature.

Several MPPT search algorithms have been proposed that make use of different characteristics of PV modules and the location of the MPP. Review articles have covered various MPPT techniques very extensively with classification and the merits and demerits of each technique [3,95]. The MPPT techniques were classified into two categories, one which needed a prior knowledge of the PV characteristics, known as indirect control or quasi-seeking methods. This includes the curve fitting method, look up table method, open-circuit voltage and short-circuit current based methods. The other category did not require any prior knowledge of PV parameters and used direct voltage or current measurements. These methods

Table 3
MPPT techniques and their characteristics.

Sl no.	MPPT techniques & references	Sensed parameters	Analog or digital implementation?	PV module parameters dependent?
1.	Hill climbing [97,98]	Voltage and current	Both	No
2.	Perturb and Observe (P&O) [99,100]	Voltage and current	Both	No
3.	Incremental conductance (INC) [101,102]	Voltage and current	Digital	No
4.	Open circuit voltage [103,104]	Voltage	Both	Yes
5.	Short circuit current [104,105]	Current	Both	Yes
6.	Artificial intelligence based techniques [106–108]	Depends on the method adopted	Digital	Yes

are known as direct control or true-seeking methods and include hill climbing, perturb and observe (P&O), incremental conductance (INC), feedback control and other similar methods. Apart from these two categories, artificial intelligence based MPPT techniques have come up in recent years and have given promising results. Table 3 describes some of the major characteristics of few popularly used MPPT techniques available in the literature [96].

Faranda et al. [109] compared 10 MPPT algorithms based on their performance and implementation costs. The algorithms were simulated and tested on a dc/dc single ended primary inductor converter (SEPIC) for a grid connected PV system using Simulink. The optimized P&O and the classical INC algorithm were found to give the best results. Berrera et al. [110] tested seven MPPT algorithms experimentally by implementing them in a boost converter. The algorithms were evaluated based on the total power and energy produced by the module in the same test cycle. The PV modules were exposed to varying artificial irradiance and it was observed that the modified P&O algorithm gave better results compared to the other methods.

The batteries connected in HRES generally require a bi-directional converter for charging and discharging purposes. Excess power from the renewable is fed into the battery bank charging. When there is deficit of power the batteries discharge and power is supplied to the load. This process involves sophisticated converters and control mechanisms to take care of battery voltage and current during the charging/discharging process. Similarly, FCs need dc–dc converters which can either buck or boost its output voltage level to interface with load or battery bank.

Jiang and Dougal [111] proposed a scheme for FC/Battery/Super capacitor hybrid system using boost converter for fuel cell and bi-directional converters for battery and super capacitor. This improved the peak power capacity of the system and provided faster response despite the slow dynamics of the fuel cell. The bi-directional converters are controlled by hysteresis current controllers. The FC current is also controlled using a PID controller along with a PWM generator. Qiang et al. [112] simulated and proposed a novel multi input, four directional dc–dc converter along with a high frequency transformer for a wind/PV/Battery hybrid system. They suggested 10 operating modes due to different combinations of the sources, storage and load. A phase shifted PWM and dual PI control scheme was used to extract the maximum power and to control the output voltage. Chuang and Ke [113] suggested a high efficiency battery charger using a zero voltage switching (ZVS) resonant converter. This charger reduces the switching losses and its operating temperature is much less compared to conventional PWM converters.

4. Optimal energy flow management in hybrid systems

An optimal energy flow management among the various energy sources in HRES is necessary since, the power output from renewable sources is intermittent and dependent on several uncontrolled conditions. The dynamic interaction between various energy sources and the loads often requires a careful study of the transient response of such systems. The energy management strategy should ensure high system efficiency and high reliability with least cost. The main objective of the technique should be to supply the peak load demand at all times. In hybrid PV systems, FCs serve as long term energy storage option and are in demand because of multiple advantages [114,115]. However the slow dynamics of FCs and its degradation due to frequent start-up and shut down cycles is a major disadvantage. Hence batteries are used in such hybrid systems to take care of power deficits and to act as a short term energy storage medium. The combination of FCs and batteries along with PV helps in ensuring uninterrupted power supply to the load.

The key parameters that influence or help in deciding the optimal energy management strategy have been summarized as follows:

- Useful electrical energy available from the primary renewable energy sources, such as solar PV and wind turbines.
- Capital cost, operating cost, lifetime and days of autonomy of storage devices, such as batteries, ultra-capacitors and FCs.
- State of charge of storage devices or the pressure level of hydrogen tanks in case of hydrogen energy systems.
- The number of start-up and shut down cycles for FCs and electrolyzer.
- Fuel price in case of hybrid systems involving DG.

The literature on energy management schemes is quite extensive and includes various configurations of the hybrid systems involving solar PV. Ipsakis et al. [116] proposed three power management strategies (PMS) for a hybrid PV/Wind/FC/Battery system with hydrogen production using electrolyzers. The PMSs are compared based on a sensitivity analysis by considering several parameters such as SOC of batteries and output power from FC. The key decision factors in the PMSs are the power delivered by the renewable energy sources and the SOC of the batteries. These PMSs strongly affect the lifetime of various subsystems, mainly the FC and electrolyzer. Three stand-alone hybrid PV systems (PV/Battery, PV/FC, PV/FC/Battery) using different energy storage technologies are discussed, analyzed and compared in [17]. The energy management strategy here is based on the system energy balance throughout the year and a trade-off between maximum system efficiency and minimum system cost has been implemented. The PV/FC/Battery hybrid system was found to have higher system efficiency with lower cost and also required lesser number of PV modules as compared to the other two configurations.

Kang and Won [117] suggested a PMS for a PV/FC/Battery hybrid system based on the cost of battery and FC. The authors have aimed at reducing the number of change over between FC and battery by introduction of measuring and time delay elements to the conventional strategy. Jiang [118] presented an effective energy management strategy and simulated in virtual test bed (VTB) environment for a PV/FC/Battery system connected to the dc bus through appropriate dc–dc power converters and controls. The PV-Battery subsystem was controlled in two modes, namely the MPPT mode and the bus (battery) voltage limit (BVL) mode. The BVL mode prevents the battery from overcharging and the MPPT mode draws maximum power from the PV module. Similarly, another

control strategy was designed to manage the FC output current through a boost converter and regulate the bus (battery) voltage by a PID controller.

Some studies on hybrid PV systems have also considered the use of UC instead of batteries [11,119]. Uzunoglu et al. [77] proposed a control strategy for a hybrid PV/FC/UC system. The UC bank stores the excess energy from PV and delivers it to the load when the FC is operating at its lower limit. The UC bank compensates the tracking mismatches and delays of the FC system, which generally exhibits a slower response. A similar strategy is suggested in [120], but the primary source of power is provided from both solar PV and wind.

Dispatch strategies for a PV/DG/Battery system based on set point values of system load and battery SOC has been proposed in [88] and an optimum set of points for starting and stopping the DG were determined. An operational control of PV/DG/Battery hybrid system to minimize the cost of fuel and storage capacity of battery has been proposed by Park et al. [121]. The authors have suggested six operating modes where the DG is either switched off or operates between constant output/maximum output depending on the battery storage energy.

5. Challenges and future trends in HRES

HRES have come a long way in terms of research and development. However, there are still certain challenges in terms of their efficiency and optimal use. The challenges faced by the developers are following:

- The renewable energy sources, such as solar PV and FCs, need break-through technology to harness more amount of useful power from them. The poor efficiency of solar PV is a major impediment in encouraging its use.
- The manufacturing cost of renewable energy sources needs a significant reduction because the high capital cost leads to an increased payback time. Cost reduction will provide an incentive to the industry to implement such systems.
- The losses involved in power electronic converters have been reduced to a satisfactory level; however, it should be ensured that there is minimal amount of power loss in these converters.
- The storage devices, such as batteries and UCs, need to increase their life-cycle through innovative technologies.
- Generation or storage of hydrogen is very expensive and energy intensive currently. There is a need of alternatives like fuel reformers based on easily available and low cost fuels.
- The implementation of HRES involves certain protection issues; hence, suitable protection devices need to be installed for safety. Moreover, introducing these distributed generators will require an up gradation in the existing protection schemes.
- These standalone systems are less adaptable to load fluctuations. Large variation in load might even lead to entire system collapse.
- The disposal of storage devices, such as batteries and hydrogen tanks and safety concerns regarding the storage of hydrogen, is a major concern for the manufacturers.

Thus the researchers and engineers need to find solutions to address the above mentioned problems. Future research and development efforts can enhance the use of renewable energy sources. Improved technology and demand for renewable energy can help in reducing the cost to an extent comparable with conventional energy. Effective and optimum use of the energy sources in standalone systems can help in meeting the energy demands of remote, inaccessible areas and make them self sufficient. Government can provide carbon tax benefits to promote the use of renewable energy. More incentive based policies promoting the establishment of renewable power plants should be rolled out by the Government. This will not only encourage the use of renewable energy but will also ensure a clean and bright future for the coming generations.

Throughout the world, energy policy is developing rapidly with the aim of providing electrical energy supplies that are low or zero carbon to reduce the production of greenhouse gases and mitigate climate change. These objectives converge in the use of distributed generation: renewable and cogeneration. HRES hold promising applications in terms of distributed generation. They can be used as an alternative to grid-connected systems in remote inaccessible sites. Power can be generated based on the demand at any particular site depending on the availability of resources. This will not only reduce the grid dependence but also help us in reducing the emission levels globally. The eco-friendly nature of hybrid renewable energy systems is a major driving factor which has enhanced its application on a large scale.

6. Conclusions

This review article presents comprehensive overview of hybrid renewable energy systems (HRES) with emphasize on solar photovoltaic based stand-alone applications. Various significant aspects of such systems, such as unit sizing and optimization, modeling of system components and optimal energy flow management strategies, are specifically reviewed. Different sizing techniques have been reviewed under classification based on availability of weather data. Developments in research on modeling of hybrid energy resources (PV systems), backup energy systems (fuel cell, battery, ultra-capacitor, diesel generator) and power conditioning units (MPPT converters, buck/boost converters, battery chargers) have been reviewed. The equivalent models including several physical mechanisms of these system components have been extensively discussed with a broad classification in modeling section. The section on energy flow management has covered significant references on various methods for optimal operation and control of HRES.

The issues on economic viability and grid interconnection are the major challenges to make the HRES adaptable and sustainable. The high capital cost and low demand in solar photovoltaic and fuel cells had slowed down the large scale implementation of such hybrid systems in the past. However, recent global boost to renewable energy markets has dramatically encouraged research and development in this sector. Future trends include cutting edge technology development to increase the efficiency of such hybrid systems and encouragement in terms of its implementation. HRES has an immense potential to meet the load demand of remote, isolated sites and can contribute significantly to both rural as well as urban development. This in turn reduces the central generation capacity and increases overall system reliability. These units can supply uninterrupted power at zero emission level which is the major advantage of such systems. The widespread use of hybrid renewable energy systems will not only solve the energy issues but also ensure a green and sustainable planet.

References

[1] Lazarov VD, Notton G, Zarkov Z, Bochev I. Hybrid power systems with renewable energy sources types, structures, trends for research and development. In: Proc of International Conference ELMA. 2005. p. 515–20.
[2] Nayar CV. Stand alone wind/diesel/battery hybrid energy systems. Wind Energy 1997;21(1):13–9.
[3] Salas V, Olias E, Barrado A, Lazaro A. Review of the maximum power point tracking algorithms for stand-alone photovoltaic systems. Sol Energ Mater Sol Cells 2006;90(11):1555–78.
[4] Chen YM, Lee CH, Wu HC. Calculation of the optimum installation angle for fixed solar-cell panels based on the genetic algorithm and the simulated-annealing method. IEEE Trans Energ Convers 2005;20(2):467–547.
[5] Rehman S, Al-Hadhrami LM. Study of a solar PV-diesel-battery hybrid power system for a remotely located population near Rafha, Saudi Arabia. Energy 2010;35(12):4986–95.

[6] Yamegueu D, Azoumah Y, Py X, Zongo N. Experimental study of electricity generation by solar PV/diesel hybrid systems without battery storage for off-grid areas. Renew Energ 2011;36(6):1780–7.
[7] Wichert B. PV-diesel hybrid energy systems for remote area power generation – A review of current practice and future developments. Renew Sust Energ Rev 1997;1(3):209–28.
[8] Hrayshat ES. Techno-economic analysis of autonomous hybrid photovoltaic-diesel-battery system. Energ Sustain Dev 2009;13(3):143–50.
[9] Solano-Peralta M, Moner-Girona M, van Sark W GJHM, Vallve X. 'Tropicalisation' of Feed-in Tariffs: a custom-made support scheme for hybrid PV/diesel systems in isolated regions. Renew Sust Energ Rev 2009;13(9):2279–94.
[10] Onar OC, Uzunoglu M, Alam MS. Dynamic modeling, design and simulation of a wind/fuel cell/ultra-capacitor-based hybrid power generation system. J Power Sources 2006;161(1):707–22.
[11] Burke A. Ultracapacitors: why, how, and where is the technology. J Power Sources 2000;91(1):37–50.
[12] Erdinc O, Uzunoglu M. Recent trends in PEM fuel cell-powered hybrid systems: Investigation of application areas, design architectures and energy management approaches. Renew Sust Energ Rev 2010;14(9):2874–84.
[13] Rahman S, Kwa-sur T. A feasibility study of photovoltaic-fuel cell hybrid energy system. IEEE Trans Energ Convers 1988;3(1):50–5.
[14] Esser T. Fuel cells enabling renewable off-grid solutions. In: IEEE 30th International Telecommunications Energy Conference, INTELEC. 2008. p. 1–2.
[15] Markvart T, Castañer L. Practical handbook of photovoltaics: fundamentals and applications. Elsevier; 2003.
[16] Mellit A, Kalogirou SA, Hontoria L, Shaari S. Artificial intelligence techniques for sizing photovoltaic systems: a review. Renew Sust Energ Rev 2009;13(2):406–19.
[17] Li C-H, Zhu X-J, Cao G-Y, Sui S, Hu M-R. Dynamic modeling and sizing optimization of stand-alone photovoltaic power systems using hybrid energy storage technology. Renew Energ 2009;32(3):815–26.
[18] Zhou K, Ferreira JA, de Haan SWH. Optimal energy management strategy and system sizing method for stand-alone photovoltaic-hydrogen systems. Int J Hydrogen Energy 2008;33(2):477–89.
[19] Ardakani FJ, Riahy G, Abedi M. Design of an optimum hybrid renewable energy system considering reliability indices. In: 18th Iranian Conference on Electrical Engineering (ICEE). 2010. p. 842–7.
[20] Xu D, Kang L, Chang L, Cao B. Optimal sizing of standalone hybrid wind/PV power systems using genetic algorithms. Canadian Conference on Electrical and Computer Engineering 2005:1722–5.
[21] Moriana I, San Martiĭn I, Sanchis P. Wind-photovoltaic hybrid systems design. In: International Symposium on Power Electronics Electrical Drives Automation and Motion (SPEEDAM). 2010. p. 610–5.
[22] Nelson DB, Nehrir MH, Wang C. Unit sizing of stand-alone hybrid wind/PV/fuel cell power generation systems. In: IEEE Power Engineering Society Gen Meet. 2005. p. 2116–22.
[23] Mellit A, Benghanem M, Hadj Arab A, Guessoum A. Modelling of sizing the photovoltaic system parameters using artificial neural network. In: Proc. of IEEE Conference on Control Applications CCA, vol. 1. 2003. p. 353–7.
[24] Senjyu T, Hayashi D, Yona A, Urasaki N, Funabashi T. Optimal configuration of power generating systems in isolated island with renewable energy. Renew Energ 2007;32(11):1917–33.
[25] Koutroulis E, Kolokotsa D, Potirakis A, Kalaitzakis K. Methodology for optimal sizing of stand-alone photovoltaic/wind-generator systems using genetic algorithms. Sol Energy 2006;80(9):1072–88.
[26] Hontoria L, Aguilera J, Zufiria P. A new approach for sizing stand alone photovoltaic systems based in neural networks. Sol Energy 2005;78(2):313–9.
[27] Mellit A, Benghanem M, Hadj Arab A, Guessoum A, Moulai K. Neural network adaptive wavelets for sizing of stand-alone photovoltaic systems. Proc of 2nd International IEEE Conference on Intelligent Systems 2004;1:365–70.
[28] Mellit A. ANFIS-based genetic algorithm for predicting the optimal sizing coefficient of photovoltaic supply (PVS) systems. In: Proc. of the Third International Conference on Thermal Engineering: Theory and Applications. 2007. p. 96–102.
[29] Notton G, Lazarov V, Zarkov Z, Stoyanov L. Optimization of hybrid systems with renewable energy sources: trends for research. In: First International Symposium on Environ Identities and Mediterranean Area, ISEIMA. 2006. p. 144–9.
[30] Agustin JLB, Lopez RD. Simulation and optimization of stand-alone hybrid renewable energy systems. Renew Sust Energ Rev 2009;13(8):2111–8.
[31] Wang L, Singh C. Compromise between cost and reliability in optimum design of an autonomous hybrid power system using mixed-integer PSO algorithm. In: International Conference on Clean Electrical Power, ICCEP. 2007. p. 682–9.
[32] Dalton GJ, Lockington DA, Baldock TE. Feasibility analysis of stand-alone renewable energy supply options for a large hotel. Renew Energ 2008;33(7): 1475–90.
[33] Shaahid SM, Elhadidy MA. Technical and economic assessment of grid-independent hybrid photovoltaic-diesel-battery power systems for commercial loads in desert environments. Renew Sust Energ Rev 2007;11(8): 1794–810.
[34] Ashok S. Optimised model for community-based hybrid energy system. Renew Energ 2007;32(7):1155–64.
[35] HOMER, http://www.homerenergy.com/ (accessed 5.2.11).
[36] HYBRID2, http://www.ceere.org/rerl/projects/software/hybrid2/download.html (accessed 5.2.11).
[37] PVSOL, http://www.valentin.de/en/downloads/products (accessed 5.2.11).
[38] RAPSIM, http://about.murdoch.edu.au/synergy/9803/rapsim.html (accessed 5.2.11).
[39] TRNSYS, http://sel.me.wisc.edu/trnsys/ (accessed 5.2.11).
[40] Villalva MG, Gazoli JR, Filho ER. Modeling and circuit based simulation of photovoltaic arrays. In: Brazilian Power Electronics Conference, COBEP. 2009. p. 1244–54.
[41] Duffie JA, Beckman WA. Solar engineering of thermal processes. third ed. Wiley; 2006.
[42] Masters GM. Renewable and efficient electric power systems. Wiley-IEEE; 2004.
[43] Tan YT, Kirschen DS, Jenkins N. A model of PV generation suitable for stability analysis. IEEE Trans Energ Convers 2004;19(4):748–55.
[44] Xiao W, Dunford WG, Capel A. A novel modeling method for photovoltaic cells. In: Proc. IEEE 35th Annual Power Electronics Specialists Conference, PESC, vol. 3. 2004. p. 1950–6.
[45] Green MA. Solar cells: Operating principles, technology and system applications. Prentice-Hall; 1982.
[46] Gow JA, Manning CD. Development of a photovoltaic array model for use in power electronics simulation studies. IEE Proc Electric Power Appl 1999;146(2):193–200.
[47] Hyvarinen J, Karila J. New analysis method for crystalline silicon cells. In: Proc of 3rd World Conference on Photovolt Energy Convers, vol. 2. 2003. p. 1521–4.
[48] Gow JA, Manning CD. Development of a model for photovoltaic arrays suitable for use in simulation studies of solar energy conversion systems. In: Proc. of 6th International Conference on Power Electronics and Variable Speed Drives. 1996. p. 69–74.
[49] Nishioka K, Sakitani N, Uraoka Y, Fuyuki T. Analysis of multicrystalline silicon solar cells by modified 3-diode equivalent circuit model taking leakage current through periphery into consideration. Sol Energ Mater Sol Cells 2007;91(13):1222–7.
[50] Ulleberg Ø, Standalone power systems for the future: optimal design, operation and control of solar hydrogen system, Ph.D. Thesis, NUST; 1998.
[51] Andujar JM, Segura F. Fuel cells: history and updating. A walk along two centuries. Renew Sust Energ Rev 2009;13(9):2309–22.
[52] Nehrir MH, Wang C. Modeling and control of fuel cells: distributed generation applications. Wiley-IEEE; 2009.
[53] Larminie J, Dicks A. Fuel cell systems explained. 1st ed. Wiley; 2000.
[54] Cheddie D, Munroe N. Review and comparison of approaches to proton exchange membrane fuel cell modeling. J Power Sources 2005;147(1–2): 72–84.
[55] Standaert F, Hemmes K, Woudstra N. Analytical fuel cell modeling. J Power Sources 1996;63(2):221–34.
[56] Standaert F, Hemmes K, Woudstra N. Analytical fuel cell modeling; non-isothermal fuel cells. J Power Sources 1998;70(2):181–99.
[57] Puranik SV, Keyhani A, Khorrami F. State-space modeling of proton exchange membrane fuel cell. IEEE Trans Energ Convers 2010;25(3):804–13.
[58] Wang C, Nehrir MH, Shaw SR. Dynamic models and model validation for PEM fuel cells using electrical circuits. IEEE Trans Energ Convers 2005;20(2):442–51.
[59] Bernardi DM, Verbrugge MW. Mathematical model of a gas diffusion electrode bonded to a polymer electrolyte. Am Inst Chem Eng J 1991;37(8): 1151–63.
[60] Bernardi DM, Verbrugge MW. A mathematical model of the solid polymer electrolyte fuel cell. J Electrochem Soc 1992;139(9):2477–91.
[61] Amphlett JC, Mann RF, Reppley BA, Roberge PR, Rodrigues A. A model predicting transient responses of proton exchange membrane fuel cells. J Power Sources 1996;61:183–8.
[62] Yerramalla S, Davari A, Feliachi A, Biswas T. Modeling and simulation of the dynamic behavior of a polymer electrolyte membrane fuel cell. J Power Sources 2003;124(1):104–13.
[63] Sharifi Asl SM, Rowshanzamir S, Eikani MH. Modeling and simulation of the steady-state and dynamic behavior of a PEM fuel cell. Energy 2010;35:1633–46.
[64] Sousa Jr R, Gonzalez ER. Mathematical modeling of polymer electrolyte fuel cells. J Power Sources 2005;147(1–2):32–45.
[65] Lebbal ME, Lecoeuche S. Identification and monitoring of a PEM electrolyser based on dynamical modelling. Int J Hydrogen Energy 2009;34(14):5992–9, 2nd International Conference on Hydrogen Safety.
[66] Moschetto A, Giaquinta G, Tina G. Modelling of integrated renewable energy systems supported by hydrogen storage. IEEE Lausanne Power Tech 2007:2088–92.
[67] Jalilzadeh S, Rohani A, Kord H, Nemati M. Optimum design of a hybrid photovoltaic/fuel cell energy system for stand-alone applications. In: 6th International Conference on Electrical Engineering/Electronics, Computer, Telecommunications and Information Technology, ECTI-CON, vol. 1. 2009. p. 152–5.
[68] Pedrazzi S, Zini G, Tartarini P. Complete modeling and software implementation of a virtual solar hydrogen hybrid system. Energ Convers Manage 2010;51(1):122–9.
[69] Zhou T, Francois B. Modeling and control design of hydrogen production process for an active hydrogen/wind hybrid power system. Int J Hydrogen Energy 2009;34(1):21–30.
[70] Raju M, Ortmann JP, Kumar S. System simulation model for high-pressure metal hydride hydrogen storage systems. Int J Hydrogen Energy 2010;35(16):8742–54.

[71] Guizzi GL, Manno M, Falco MD. Hybrid fuel cell-based energy system with metal hydride hydrogen storage for small mobile applications. Int J Hydrogen Energy 2009;34(7):3112–24.
[72] Zini G, Tartarini P. Wind-hydrogen energy stand-alone system with carbon storage: modeling and simulation. Renew Energ 2010;35(11):2461–7.
[73] Thounthong P, Chunkag V, Sethakul P, Sikkabut S, Pierfederici S, Davat B. Energy management of fuel cell/solar cell/supercapacitor hybrid power source. J Power Sources 2011;196:313–24.
[74] Khan MJ, Iqbal MT. Dynamic modeling and simulation of a small wind-fuel cell hybrid energy system. Renew Energ 2005;30(3):421–39.
[75] Spyker RL, Nelms RM. Classical equivalent circuit parameters for a double-layer capacitor. IEEE Trans Aerosp Electron Syst 2000;36(3):829–36.
[76] Shi L, Crow ML. Comparison of ultracapacitor electric circuit models. In: IEEE Power and Energy Society Gen. Meeting – Convers. and Delivery of Electrical Energy in the 21st Century. 2008. p. 20–4.
[77] Uzunoglu M, Onar OC, Alam MS. Modelling, control and simulation of a PV/FC/UC based hybrid power generation system for stand-alone applications. Renew Energ 2009;34:509–20.
[78] Spyker RL, Nelms RM. Analysis of double-layer capacitors supplying constant power loads. IEEE Trans Aerosp Electron Syst 2000;36(4):1439–43.
[79] Salameh ZM, Casacca MA, Lynch WA. A mathematical model for lead-acid batteries. IEEE Trans Energ Convers 1992;7(1):93–8.
[80] Saiju R, Heier S. Performance analysis of lead acid battery model for hybrid power system. In: IEEE/PES Transmission and Distribution Conference and Exposition. 2008. p. 1–6.
[81] Marchetti GP, Piccolo M. Mathematical models for the construction of a renewable energy hybrid plant. In: 12th International Telecommunications Energy Conference, INTELEC. 1990. p. 502–9.
[82] Arun P, Banerjee R, Bandyopadhyay S. Optimum sizing of battery-integrated diesel generator for remote electrification through design-space approach. Energy 2008;33:1155–68.
[83] Fung C, Wiengmoon B, Nayar CV. An investigation on the characteristics and performance of a PV-diesel hybrid energy system for teaching and research. In: Proc of IEEE Region 10 Conference on Computers, Communications, Control and Power Engineering TENCON, vol. 3. 2002. p. 1962–5.
[84] Dufo-Loïpez R, Bernal-Agustin JL. Multi-objective design of PV- wind-diesel-hydrogen- battery systems. Renew Energ 2008;33:2559–72.
[85] Ponnambalam K, Saad YE, Mahootchi M, Heemink AW. Comparison of methods for battery capacity design in renewable energy systems for constant demand and uncertain supply. In: 7th International Conference on the European Energy Market (EEM). 2010. p. 1–5.
[86] Gupta A, Saini RP, Sharma MP. Modelling of hybrid energy system – Part 1: Problem formulation and model development. Renew Energ 2011;36:459–65.
[87] Mandi RP, Yaragatti UR. Solar PV-diesel hybrid energy system for rural applications. In: 5th International Conference on Industrial and Information Systems ICIIS. 2010. p. 602–7.
[88] Ashari M, Nayar CV. An optimum dispatch strategy using set points for a photovoltaic (pv)-diesel-battery hybrid power system. Sol Energy 1999;66(1):1–9.
[89] Ganesan V. Internal combustion engines. third ed. Tata McGraw Hill Education; 2008.
[90] Wies RW, Johnson RA, Agrawal AN, Chubb TJ. Simulink model for economic analysis and environmental impacts of a pv with diesel-battery system for remote villages. IEEE Trans Power Syst 2005;20(2):692–700.
[91] Cheong KL, Li PY, Xia J. Control oriented modeling and system identification of a diesel generator set (genset). In: American Control Conference. 2010. p. 950–5.
[92] Mirošević M, Maljković Z, Mišković M. Dynamics of diesel-generator-units during direct-on-line starting of induction motors. In: 13th European Conference on Power Electronics and Applications, EPE. 2009. p. 1–8.
[93] Mousazadeh H, Keyhani A, Javadi A, Mobli H, Abrinia K, Sharifi A. A review of principle and sun-tracking methods for maximizing solar systems output. Renew Sust Energ Rev 2009;13(8):1800–18.
[94] Bajpai P, Dash V, Kishore NK. Bi-annual sun tracking mechanism for PV module support structure: study and implementation. In: Sixteenth National Power System Conference (NPSC). 2010. p. 56–61.
[95] Desai HP, Patel HK. Maximum power point algorithm in pv generation: an overview. In: 7th International Conference on Power Electronics and Drive Systems, PEDS. 2007. p. 624–30.
[96] Esram T, Chapman PL. Comparison of photovoltaic array maximum power point tracking techniques. IEEE Trans Energ Convers 2007;22(2):439–49.
[97] Xiao W, Dunford WG. A modified adaptive hill climbing MPPT method for photovoltaic power systems. In: IEEE 35th Annual Power Electronics Specialists Conference PESC, vol. 3. 2004. p. 1957–63.
[98] Sera D, Teodorescu R, Hantschel J, Knoll M. Optimized maximum power point tracker for fast changing environmental conditions. In: IEEE International Symposium on Industrial Electronics, ISIE. 2008. p. 2401–7.
[99] Fermia N, Granozio D, Petrone G, Vitelli M. Predictive & adaptive mppt perturb and observe method. IEEE Trans Aerosp Electron Syst 2007;43(3): 934–50.
[100] Piegari L, Rizzo R. Adaptive perturb and observe algorithm for photovoltaic maximum power point tracking. Renew Power Generation, IET 2010;4(4):317–28.
[101] Xuesong Z, Daichun S, Youjie M, Deshu C. The simulation and design for MPPT of PV system based on incremental conductance method. In: WASE International Conference on Information Engineering (ICIE), vol. 2. 2010. p. 314–7.
[102] Yusof Y, Sayuti SH, Abdul Latif M, Wanik MZC. Modeling and simulation of maximum power point tracker for photovoltaic system. In: Proc. of National Power and Energy Conference, PEC. 2004. p. 88–93.
[103] Tariq A, Asghar J. Development of an analog maximum power point tracker for photovoltaic panel. In: International Conference on Power Electronics and Drives Systems, PEDS, vol. 1. 2005. p. 251–5.
[104] Yuvarajan S, Shoeb J. A fast and accurate maximum power point tracker for PV systems. In: Twenty-Third Annual IEEE Applied Power Electronics Conference and Exposition, APEC. 2008. p. 167–72.
[105] Yuvarajan S, Xu S. Photo-voltaic power converter with a simple maximum-power-point-tracker. In: Proceedings of the 2003 International Symposium on Circuits and System, ISCAS, vol. 3. 2003. p. III-399–402.
[106] Syafaruddin Karatepe E, Hiyama T. Artificial neural network-polar coordinated fuzzy controller based maximum power point tracking control under partially shaded conditions. Renew Power Generation, IET 2009;3(2): 239–53.
[107] D'Souza NS, Lopes LAC, Liu X. An Intelligent maximum power point tracker using peak current control. In: IEEE 36th Power Electronics Specialists Conference, PESC. 2005. p. 172.
[108] Subiyanto, Mohamed A, Hannan MA. Hardware implementation of fuzzy logic based maximum power point tracking controller for PV systems. In: 4th International Power Engineering and Optimization Conference (PEOCO). 2010. p. 435–9.
[109] Faranda R, Leva S, Maugeri V. MPPT techniques for PV Systems: energetic and cost comparison. In: IEEE Power and Energy Society Gen. Meeting – Convers and Delivery of Electrical Energy in the 21st Century. 2008. p. 1–6.
[110] Berrera M, Dolara A, Faranda R, Leva S. Experimental test of seven widely adopted MPPT algorithms. IEEE Bucharest Power Tech 2009:1–8.
[111] Jiang Z, Dougal RA. A hybrid fuel cell power supply with rapid dynamic response and high peak-power capacity. In: Twenty-First Annual IEEE Applied Power Electronics Conference and Exposition APEC. 2006. p. 6.
[112] Qiang M, Wei-yang W, Zhen-lin X. A multi-directional power converter for a hybrid renewable energy distributed generation system with battery storage. In: CES/IEEE 5th International Power Electronics and Motion Control Conference, IPEMC, vol. 3. 2006. p. 1–5.
[113] Chuang Y-C, Ke Y-L. A novel high-efficiency battery charger with a buck zero-voltage-switching resonant converter. IEEE Trans Energ Convers 2007;22(4):848–54.
[114] Ahmed NA, Miyatake M, Al-Othman AK. Power fluctuations suppression of stand-alone hybrid generation combining solar photovoltaic/wind turbine and fuel cell systems. Energ Convers Manage 2008;49(10):2711–9.
[115] El-Shatter TF, Eskander MN, El-Hagry MT. Energy flow and management of a hybrid wind/PV/fuel cell generation system. Energ Convers Manage 2006;47(10):1264–80.
[116] Ipsakis D, Voutetakis S, Seferlis P, Stergiopoulos F, Elmasides C. Power management strategies for a stand-alone power system using renewable energy sources and hydrogen storage. Int J Hydrogen Energy 2009;34(16): 7081–95.
[117] Kang K-H, Won D-J. Power management strategy of stand-alone hybrid system to reduce the operation mode changes. In: Transmission & Distribution Conference & Exposition: Asia and Pacific. 2009. p. 1–4.
[118] Jiang Z. Power management of hybrid photovoltaic – fuel cell power systems. In: IEEE Power Engineering Society Gen. Meeting. 2006. p. 6.
[119] Lajnef W, Vinassa JM, Briat O, Azzopardi S, Woirgard E. Characterization methods and modeling of ultracapacitors for use as peak power sources. J Power Sources 2007;168(2):553–60.
[120] Onar OC, Uzunoglu M, Alam MS. Modeling, control and simulation of an autonomous wind turbine/photovoltaic/fuel cell/ultra-capacitor hybrid power system. J Power Sources 2008;185(2):1273–83.
[121] Park J-S, Katagi T, Yamamoto S, Hashimoto T. Operation control of photovoltaic/diesel hybrid generating system considering fluctuation of solar radiation. Sol Energ Mater Sol Cells 2001;67(1–4):535–42.